Chapter 5

Identification of lethal microRNAs specific for head and neck cancer.

Clin Cancer Res. 2013; 19(20):5647-5657.

Marlon Lindenbergh-van der Plas
Sanne R. Martens-de Kemp
Michiel de Maaker
Wessel N. van Wieringen
Bauke Ylstra
Reuven Agami
Francesco Cerisoli
C. René Leemans
Boudewijn J.M. Braakhuis
Ruud H. Brakenhoff

ABSTRACT

Objective: The prognosis of head and neck squamous cell carcinoma (HNSCC) remains disappointing and the development of novel anti-cancer agents is urgently awaited. We identified, by a functional genetic screen, microRNAs (miRNAs) that are selectively lethal for head and neck cancer cells but not for normal cells. We further investigated the genes targeted by these miRNAs.

Methods: A retroviral expression library of human miRNAs was introduced in HNSCC cell lines and normal oropharyngeal keratinocytes to identify tumor-selective lethal miRNAs. Potential downstream gene targets of these miRNAs were identified by gene expression profiling and validated by functional assays.

Results: We identified six miRNAs that selectively inhibit proliferation of head and neck cancer cells. By gene expression profiling and 3' untranslated region (UTR) luciferase reporter assays, we showed that the ataxia telangiectasia mutated (*ATM*) gene is a common target for at least two and likely three of these miRNAs. Specific inhibition of *ATM* resulted in a similar tumor-specific lethal effect, whereas the phenotype was reverted in rescue experiments.

Conclusion: These six miRNA might be developed as novel anti-cancer agents and highlight *ATM* as an interesting novel therapeutic target for head and neck cancer.

INTRODUCTION

Head and neck squamous cell carcinoma (HNSCC) develops in the mucosal linings of the upper aerodigestive tract and contributes to approximately 5% of all cancers in the Western world[1,2]. Well-known risk factors are tobacco smoking, excessive consumption of alcohol containing beverages, and infection with the human papillomavirus (HPV)[3-5]. About one third of the patients present with early-stage tumors and receive single modality treatment, either surgery or radiotherapy. The 5-year survival rates for patients with early disease stages are more than 90%. Unfortunately the majority of patients with HNSCC present with advanced disease stages. These patients are treated with either a combination of surgery and radiotherapy or chemoradiation, the concurrent application of systemic cisplatin chemotherapy combined with locoregional radiotherapy. Patients with advanced disease stages frequently develop locoregional recurrences, distant metastasis, and/or second primary tumors, which results in 5-year survival rates of less than 60%[1]. Therefore, the development of novel anti-cancer agents to improve outcome is urgently awaited.

MicroRNAs (miRNAs) are ~22 nucleotide long, non-coding RNAs that are able to regulate the expression of multiple target genes[6]. Classically, miRNAs regulate the expression of target genes through sequence-specific complementarity between the miRNA seed sequence and the 3' untranslated region (UTR) of the target mRNAs[7]. Perfect complementarity between the miRNA and the mRNA will generally target the mRNA for degradation, whereas imperfect complementarity of the miRNA to the 3'UTR will preferentially repress mRNA translation[8]. However, insights on the interaction of miRNAs with their target genes evolve continuously. Through this regulation at the posttranscriptional level, miRNAs are able to modulate the expression of numerous genes simultaneously, thereby regulating individual signaling pathways at multiple levels[9].

Several studies have shown the importance of miRNAs in cancer, including HNSCCs. Altered miRNA expression profiles have been observed in both HNSCC cell lines and tumors when compared to the normal counterpart tissues[10,11]. The overexpression of miR-21 is described in many tumor types, including HNSCCs. Moreover, overexpression of miR-21 also increased with a higher grade of preneoplastic lesions during malignant progression[10]. A number of these differentially expressed miRNAs were shown to be associated with poor prognosis, such as miR-21 and miR-211[12,13]. Even more interestingly, recent studies have revealed that miRNAs may act as tumor suppressors by targeting oncogenes. For example, the miR-16 family inhibits cell cycle progression and induces apoptosis via the silencing of *BCL2*[14], described in multiple tumor types, including HNSCC. In a similar manner, ectopic expression of miR-181a resulted in decreased proliferation by targeting the oncogene *KRAS*[15].

In the present study, we examined the potential of miRNAs for treatment of HNSCCs. We hypothesized that miRNAs might cause tumor-specific cell death in HNSCCs by targeting genes that might show a synthetic lethal interaction with one or more inactivated cancer genes. Several tumor-suppressing routes are inactivated in HNSCCs among which the p53 and pRb pathways. Other genes or signaling routes may take over part of the lost functions and show a synthetic lethal interaction when inhibited[16]. We used a human miRNA expression library in retroviral vectors to conduct a functional genetic screen to specifically identify miRNAs that cause cell death of tumor cells and not of primary keratinocytes. We further investigated, by expression array analysis, the target genes of these miRNAs as functional inhibition of the target genes may elicit the same lethal phenotype and could be performed by small molecules.

MATERIAL AND METHODS

Cell culture

Normal oral or oropharyngeal keratinocytes were isolated and cultured as previously described[17]. Conditionally immortalized oropharyngeal keratinocytes (ciOKC) were generated by transformation of primary oropharyngeal keratinocytes with a temperature-sensitive SV40 large T-antigen. Primary keratinocytes and ciOKCs were cultured in Keratinocyte Serum Free Medium (KSFM; Invitrogen) supplemented with 0.1% bovine serum albumin, 25 mg bovine pituitary extract, 2.5 µg human recombinant EGF, 250 µg Amphotericin B (MP biomedicals) and 250 µg gentamycin (Sigma-Aldrich) at 32°C[18]. VU-SCC-120, VU-SCC-OE, UM-SCC-6, SiHa, MCF7, HT29, U87, HEK293T and Phoenix cells were cultured in Dulbecco's Modified Eagles' Medium (DMEM), 5% FCS, 2 mM L-glutamine, 50 U/ml Penicillin and 50 µg/ml Streptomycin at 37°C and 5% CO_2. The HNSCC cell lines used were all negative for the human papillomavirus and were sequenced for *TP53* mutations. Cell line UM-SCC-6 was *TP53* wild type, VU-SCC-120 contained two missense mutations (c.181_182CG>TT and c.527G>A) and VU-SCC-OE a truncating deletion (c.11_919del). Cell lines are authenticated regularly by their morphological characteristics and analysis of *TP53* mutations and genetic markers.

Functional screen of human miRNA library

Amphotropic retroviral supernatants were produced for 370 annotated and putative miRNAs included in the human miRNA expression library (miR-Lib) with miR-Vec-Ctrl (scrambled sequence) as negative control[18,19]. The conditionally immortalized oropharyngeal keratinocytes were used for screening experiments as described previously[18]. CiOKC and VU-SCC-120 cells (HNSCC cell line previously described as 93VU120[20]) were transduced for 24 hours (VU-SCC-120) or at two following days for four hours (ciOKC) in the presence of 3 µg/ml polybrene (Sigma-Aldrich). After 48 hours, the cells were subjected to blasticidin selection. For ciOKC this was two days 4 µg/ml and subsequently 5 days of 8 µg/ml blasticidin (Sigma-Aldrich). For VU-SCC-120 the selection was conducted with 10 µg/ml for four days. For the initial screen, cell survival was assessed by visual inspection when the negative control (miR-Vec-Ctrl) had reached 100% confluency and expressed as estimated percentage of the control (Supplementary Table S1). For subsequent validation experiments, cell viability was quantified using the CellTiter-Blue Cell Viability Assay (Promega). The conversion of resazurin to resorufin was measured using the Infinite 200 plate reader (Tecan Group Ltd).

RNA isolation from formalin-fixed, paraffin-embedded tissue

Normal oropharyngeal mucosa was derived from three formalin-fixed, paraffin-embedded (FFPE) specimens from patients who underwent uvulopalatopharyngoplasty. In addition, FFPE tumor biopsies were obtained from five patients with HNSCC. The mucosal epithelium was microdissected from sections of the uvula specimen as previously described[21]. Likewise, neoplastic areas were microdissected from tumor samples. Microdissected tissues were treated with 1 mg/ml of proteinase K for 17 hours at 56°C in buffer containing 100 mM Tris-HCl (pH 9.0), 10 mM NaCl, 1% SDS and 5 mM EDTA (pH 8.2). Nucleic acids were isolated by phenol-chloroform extraction and precipitated by sodium acetate and ethanol according to standard protocols using glycogen as carrier. After the nucleic acids were washed with 70% ethanol, they were redissolved in RNAse-free water.

Lentiviral shRNA ATM transduction

Lentiviral vectors with short-hairpin RNA (shRNA) sequences targeting *ATM* transcripts were obtained from the MISSION short-hairpin library of The RNAi Consortium (Sigma-Aldrich) that is available at VU University Medical Center. Viral supernatants were produced by cotransfection of HEK239T cells using FuGENE 6 (Roche diagnostics) with the pLKO.1 short-hairpin vector

together with the packaging and envelop vectors. Both ciOKC and VU-SCC-120 (HNSCC cell line) were transduced with lentiviruses at two following days for four hours in the presence of 3 μg/ml polybrene (Sigma-Aldrich). In total 48 hours after transduction, cells were subjected to puromycin selection (Sigma Aldrich). For ciOKC, this was two days of 5 μg/ml and subsequently 5 days of 10 μg/ml, and for VU-SCC-120 the selection was conducted with 1 μg/ml for seven days.

Quantitative Reverse Transcription-PCR

Total RNA was isolated using the mirVana miRNA Isolation Kit (Ambion) according to the instructions of the manufacturer with the only modification that columns were eluted with 2x 25 μl elution buffer. Expression of hsa-miR-181a, hsa-miR-323, hsa-miR-326, hsa-miR-342, hsa-miR-345 and hsa-miR-371 was analyzed by Taqman miRNA assays following the instructions of the manufacturer (Applied Biosystems). *ATM* expression was analyzed by Taqman gene expression assay. Relative expression was calculated via the comparative C_t method using the small nucleolar RNA transcript RNU44 (for miRNA analysis) or beta-glucuronidase (*BGUS:* for *ATM* analysis) as internal references[22]. Quantitative RT-PCR reactions without reverse transcriptase were carried out in parallel for each RNA sample to exclude signal produced by contaminating genomic DNA.

Gene expression profiling

The retroviral clones with miRNA genes miR-181a, miR-323, miR-326, miR-342, miR-345 and miR-371 and negative control miR-Vec-Ctrl were transiently transfected in VU-SCC-120 by FuGENE 6 (Roche diagnostics). Total RNA was isolated 72 hours after transfection using the mirVana miRNA Isolation Kit (Ambion). Microarray hybridization using the Agilent Low Input Quick Amplification Labeling Kit and 4x44K Whole Human Genome Arrays was carried out according to the manufacturer (Agilent Technologies). Normalization of the gene expression data was conducted within R statistical software using the Limma package and comprised of RMA background correction, loess within-array normalization, and A-quantile between-array normalization. Then, missing values were imputed using the impute-package (impute.knn with default settings). Finally, the slide and dye effects were removed by gene-wise linear regression using the log-intensity values.

The log fold changes between the reference group and each treated group were used to cluster the six treatments. This was carried out by means of hierarchical clustering with ward linkage, and the similarity defined both as the Euclidean distance and as one minus the absolute value of the Spearman rank correlation measure. The grouping from hierarchical clustering was verified by means of principal component plots. Within each cluster, the differences in gene expression between reference and treated samples were evaluated by means of a *t* test. The multiplicity problem (many genes were tested) was addressed by application of the Benjamini-Hochberg procedure to the raw *P* values to control the False Discovery Rate (FDR). Data are accessible under GEO number GSE34881.

ATM inhibitor treatment

Both ciOKC and VU-SCC-120 cells were subjected to a concentration range of 40-0.075 μM ATM inhibitor CP466722 (Axon Medchem). After 72 hours, cell viability was assessed with the CellTiter-Blue Cell Viability Assay (Promega).

ATM 3'UTR reporter luciferase assay

CiOKC cells were transiently co-transfected with a luciferase reporter construct containing the 3'UTR sequence of *ATM* (GeneCopoeia) and one of the retroviral vectors containing the miR-181a, miR-323, miR-326 genes or negative control miR-Vec-Ctrl by FuGENE 6. In total 72 hours after transfection, firefly and *Renilla* luciferase activity was measured using the LucPair miR

Dual Luciferase Assay Kit according to the instructions of the manufacturer (GeneCopoeia). Luciferase activity was measured using the Infinite 200 plate reader (Tecan Group Ltd).

Lethal phenotype rescue

VU-SCC-120 cells were transiently transfected with either pcDNA3.1(+)Flag-His-ATMwt (wild type *ATM* cDNA sequence, Addgene plasmid 31985) or pcDNA3.1(+) Flag-His-ATMkd (kinase-dead *ATM* cDNA sequence, Addgene plasmid 31986)[23]. Amphotropic retroviral supernatants were produced for miR-181a, miR-326, miR-345, and miR-Vec-Ctrl (scrambled sequence) as negative control. VU-SCC-120-ATMwt, and VU-SCC-120-ATMkd cells were transduced with the miRNA expressing retroviruses at two following days for four hours in the presence of 3 µg/ml polybrene. After 72 hours cell viability was assessed by the CellTiter-Blue cell viability assay.

RESULTS

Identification of miRNAs lethal for HNSCCs

To identify miRNAs that are lethal for head and neck cancer cells, we introduced a human miRNA expression library (miR-Lib) in HNSCC cell line VU-SCC-120 and close to normal conditionally immortalized primary oropharyngeal keratinocytes (ciOKC) (Fig. 1A). The ciOKC cells have been immortalized by a temperature-sensitive SV40 large T antigen. When cultured at 32°C, they are immortalized, while they become senescent when shifted to 39°C as a result of the inactivation of the large T-antigen. They behave, also at 32°C, as normal keratinocytes except for the immortalized phenotype[18].

The majority of miRNAs did not influence the survival of either tumor cells or ciOKC cells, or the lethal effect was similar in both models. However, a subset of 19 miRNAs (5.4%) specifically affected the head and neck cancer cell line, whereas the ciOKCs remained unaffected (Supplementary Table S1, Fig. 1B). To verify the tumor-specific lethal effect of these miRNAs, we screened all nineteen miRNAs in two different ciOKC cell clones and three HNSCC cell lines (VU-SCC-OE, UM-SCC-6 and VU-SCC-120). We could not confirm the tumor-specific lethal effect of thirteen miRNAs. The remaining six miRNAs showed the expected phenotype (Supplementary Fig. S1): a decreased proliferation in HNSCC cells, but not in ciOKC cells, and these miRNAs were further investigated. Visual inspection indicated that the tumor cells had disappeared from the wells indicating that they likely ceased proliferation and died. As yet, we did not elucidate the precise molecular mechanism behind the cell death.

For the initial large scale discovery screens we had to rely on the ciOKC cell model to study the effect of the miRNAs. In the subsequent small scale validation experiments we included primary keratinocytes. The miRNAs miR-181a, miR-323, miR-326, miR-342, miR-345 and miR-371 all showed a significant decrease in cell proliferation in three HNSCC cell lines and not or only to a limited extent in primary keratinocytes (Fig. 1C). The sequence identity of these six miRNAs was confirmed by Sanger sequencing (data not shown).

MiRNA expression in HNSCCs

As the ectopic expression of the six tumor-selective lethal miRNAs caused cell death in tumor cell lines, but not or less in mucosal keratinocytes, we were interested in the expression of these miRNAs in HNSCC tumors and normal oral mucosa. Hence, we determined expression levels for the six miRNAs in RNA extracted from both microdissected tumor and mucosal epithelium. MiR-371 was neither expressed in normal mucosa nor in the five tumors analyzed (data not shown). For the other five miRNAs, expression was observed in all tumor and mucosal epithelium samples, but apparently at a low level (Fig. 2). The expression levels of the miRNAs were in all cases lower than the expression of the RNU44 reference gene. In addition, only small differences in expression levels were observed between mucosa and tumor samples. The expression of miR-181a was slightly increased in tumors, but not significant (Fig. 2A). For miR-326, miR-342

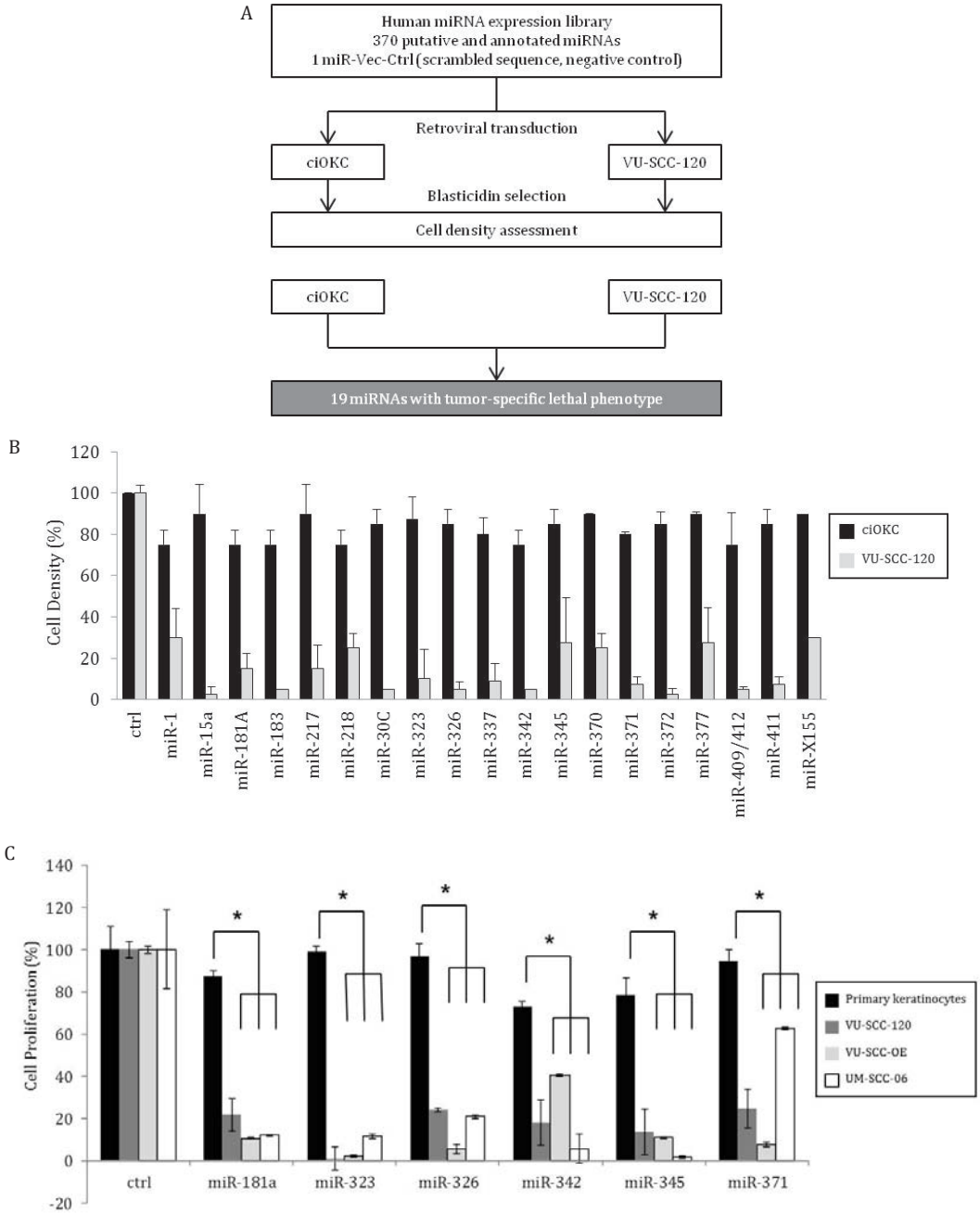

Figure 1. Identification of 19 miRNAs with a potential tumor-specific lethal effect by a functional genetic screen. (A) Schematic representation of the primary tumor-specific lethality screen. Both ciOKC and VU-SCC-120 cells were retrovirally transduced with a human miRNA expression library. After blasticidin selection of transduced cells, cell density was assessed. The miRNAs that had little to no effect on cell density (70-100%) in ciOKC cells, but did result in low cell density (0-30%) in VU-SCC-120 cells were identified as potentially tumor-specific lethal. (B) The 19 miRNAs that were selected in the initial screen showed cell survival differences between ciOKC (dark grey bars) and VU-SCC-120 (grey bars) cells. Cell density in duplicate wells was visually estimated by two independent observers, with standard deviation (SD) as error bars. (C) The effect of ectopic expression of the indicated six miRNAs on survival of primary oral keratinocytes (dark grey bars) and head and neck cancer cell lines VU- SCC-120 (medium grey bars), VU-SCC-OE (light grey bars) and UM-SCC-6 (white bars). Cell proliferation was quantified by the CellTiter-Blue Assay. The average value of triplicate experiments is shown, with SDs as error bars. Significant differences are indicated by an asterisk ($P < 0.05$, Student t test).

and miR-345 the expression level in tumor tissue was decreased when compared to normal mucosal epithelium, but not significantly. Only the expression level of miR-323 was significantly lower in tumor cells (Fig. 2B).

Tumor-specific lethal phenotype in cell lines of different cancer types

We next questioned whether the effect observed in the HNSCC cell lines was specific for HNSCCs. Therefore we tested the six miRNAs with HNSCC-specific lethal effects in other cancer cell lines. The introduction of the various miRNAs in cervical carcinoma cell line (SiHa) and breast carcinoma cell line (MCF7) had no effect on proliferation except for miRNA 181a (Supplementary Fig. S2, upper panels). However, when the miRNAs were introduced in colon adenocarcinoma cell line (HT29) or glioblastoma cell line (U87), a decrease in cell proliferation was observed, although with a less severe phenotype than the tested HNSCC cell lines (Supplementary Fig. S2, lower panels). The effects observed vary with the specific miRNA. This strongly suggests that genes are targeted that show synthetic lethal interactions in relation to the mutational status of specific cancer genes or deregulated signaling pathways in the various cell lines of different tissue origin, and it might be worthwhile to repeat these functional screens for other tumor types, as it might reveal other candidate miRNAs. The lethal interaction is likely not related to a mutation in *TP53* as all miRNAs showed the tumor-selective lethal effect in all three HNSCC cell lines, whereas one cell line was *TP53* wild-type, one showed two missense mutations and one a large deletion (see Material and Methods for details).

Target gene analysis

MiRNAs regulate gene expression at the post-transcriptional level, so we were interested in the downstream gene targets of these six tumor-specific lethal miRNAs that might explain the cell growth inhibitory phenotype. First, we conducted an *in silico* analysis. There is a multitude of software tools available for target identification (reviewed in ref. [24]), and we chose TargetScan and DIANA-microT. We also defined the overlap between genes detected by the two programs (Supplementary Table S2). There was a wide variety of potential genes identified with more

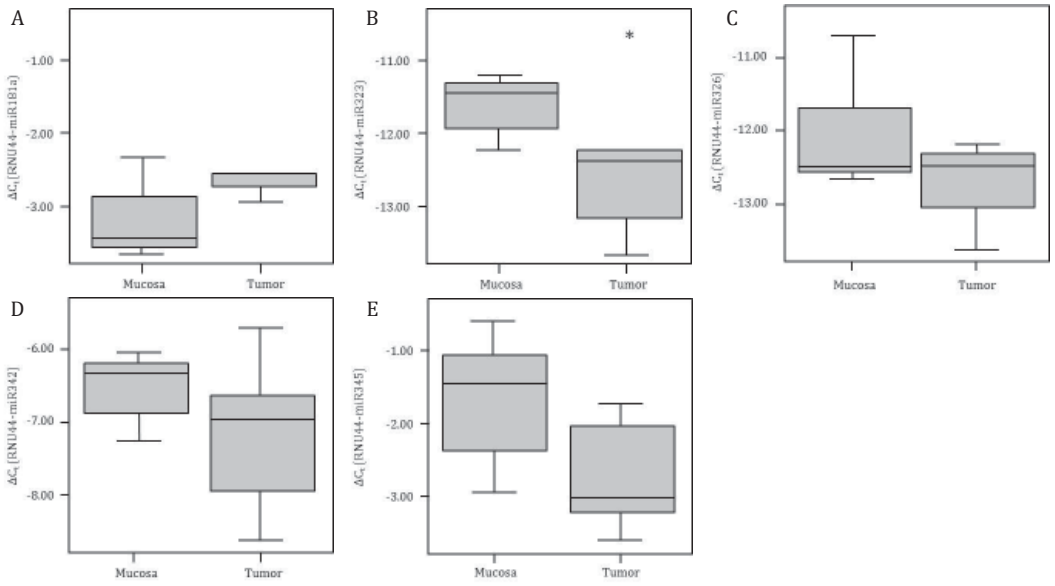

Figure 2. Box plots of the expression of the six lethal miRNAs in HNSCC tumors and normal mucosal epithelium. MiRNA levels were determined using qRT-PCR analysis on RNA of microdissected FFPE tumors and mucosal epithelium. ΔCt values, Ct(miRNA)-Ct(RNU44), are depicted for (A) miR-181a (B) miR-323 (C) miR-326 (D) miR-342 and (E) miR-345. MiR-371 was not expressed in squamous tissues. Significant differences are indicated by an asterisk (P <0.05 with Student t test).

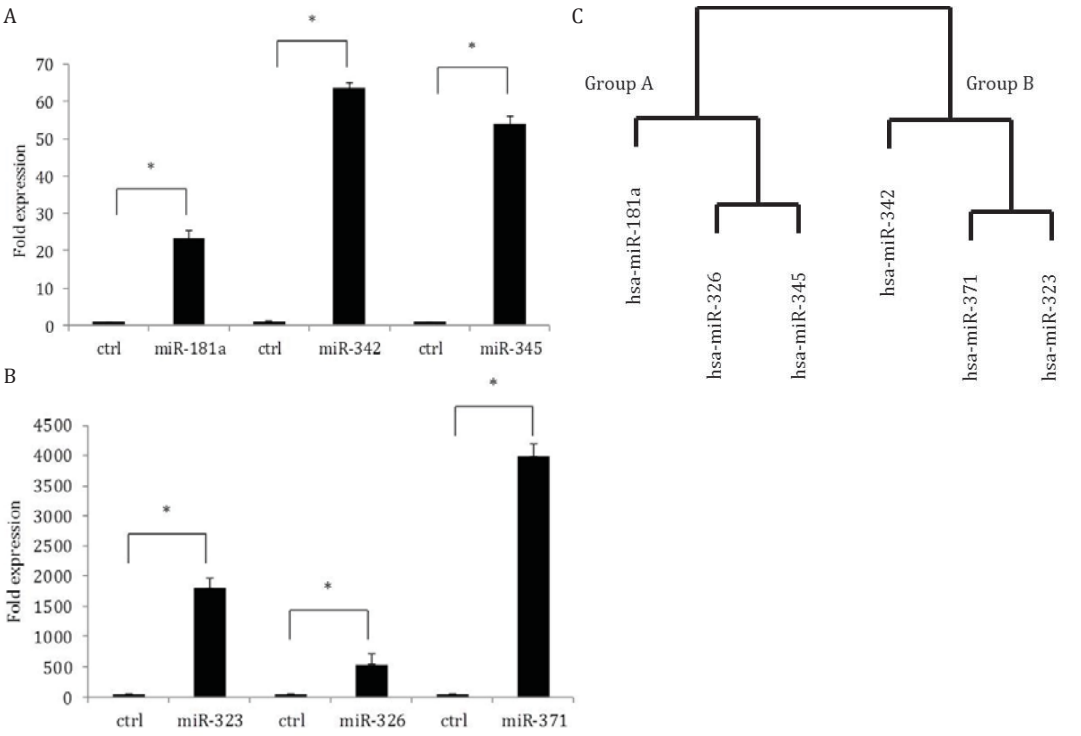

Figure 3. Ectopic expression of miRNAs and their effect on gene expression.
VU-SCC-120 cells were transiently transfected with the six different miRNA plasmids and overexpression of the indicated miRNAs was compared to miR-Vec-Ctrl transfected cells for (A) miR-181a, miR-326, and miR-345 as well as (B) miR-323, miR-326 and miR-371. Significant differences are indicated by an asterisk (P <0.05, Student t test). Two separate groups became apparent by hierarchical cluster analysis (C) after genetic expression profiling of the cells transfected with the miRNA plasmids.

than 700 for miR-181a. This analysis did not give a direct clue.
Therefore, we conducted micro-array based gene expression analysis to identify candidate target genes. As ectopic expression of these miRNAs caused a decrease in cell proliferation and cell death as phenotype in HNSCC cell lines, we were unable to analyze cells stably transduced with the miRNAs. We therefore decided to transiently transfect VU-SCC-120 cells with the retroviral vector plasmids instead of transduction with retroviral particles. Transient transfection is efficient, and overexpression can be observed almost immediately. RNA was isolated 72 hours post-transfection, the time point with high miRNA expression, but before cell death was observed (Supplementary Fig. S3). The expression level of the transfected miRNAs was also determined. Depending on the endogenous expression of the miRNAs in VU-SCC-120 cells, expression increased from 23 to 4,000 fold after transient transfection (Fig. 3A-3B).
Next, total RNA of the transfected cells was labeled and hybridized for gene expression profiling by micoarray hybridization. We assumed that some of these six miRNAs might in fact target the same genes, and we therefore focused on a groupwise comparison. In the expression profiles, we indeed observed significant correlations between miRNA associated mRNA expression profiles (Table 1). Highly significant correlations were observed for miR-181a and miR-326 (r=0.572), miR-326 and miR-345 (r=0.573), miR-323 and miR-371 (r=0.602) and miR-342 and miR-323 (r=0.577). Cluster analysis revealed two groups of each three miRNAs with downstream target effects that showed significant correlations (Fig. 3C; Supplementary Tables S3 and S4). MiR-181a, miR-326 and miR-345 clustered together in group A and group B was composed of miR-342, miR-371 and miR-323. The profiles of the miRNAs per group were combined and analyzed against the empty vector control (in tetraplicate hybridized on the arrays) to detect significant

Table 1. Correlations of gene expression profiles between different microRNAs.

	miR-181a	miR-326	miR-371	miR-345	miR-323	miR-342
miR-181a	1.000					
miR-326	0.572	1.000				
miR-371	0.113	0.119	1.000			
miR-345	0.373	0.573	0.158	1.000		
miR-323	0.099	0.087	0.602	0.170	1.000	
miR-342	0.074	0.065	0.388	0.123	0.577	1.000

differentially expressed genes.

In total we observed 187 and 15 genes (FDR corrected *P* value <0.1) that were significantly differentially expressed genes in group A and B, respectively, as compared to the empty vector control. Subsequently, we applied several rankings on the differentially expressed genes to distinguish primary effects from secondary effects. First, we selected the genes that showed a decreased level of expression, as miRNAs are considered to cause downregulation of expression of their target genes. Second, as for many genes multiple probes were present on the array, we subsequently ranked the genes based on the number of probes per gene with an FDR corrected *P* value <0.1 (Supplementary Tables S3 and S4). One of the most striking target genes, that is apparently regulated by the miRNAs from group A, is the *ATM* gene. First, the differences of many probes are highly significant given the limited sample size (four controls versus three miRNAs of group A analyzed in duplicate) and the conservative *P* value adjustment. Second, in total 9 of 12 *ATM* probes were significantly regulated. Unfortunately, we did not find such an apparent lead target for the miRNAs in group B.

Knockdown of ATM causes tumor-specific lethality

ATM is a nuclear protein kinase that senses DNA damage and activates downstream pathways[24]. To validate the observed decrease in expression, we carried out qRT-PCR for *ATM* in the same samples that were transiently transfected with the miRNAs and that were analyzed by microarray hybridization. Indeed we confirmed that *ATM* expression is inhibited in the RNA samples from group A (Fig. 4A).

As ectopic expression of miR-181a, miR-326, and miR-345 results in tumor-specific lethality and downregulation of *ATM* expression, we hypothesized that knockdown of *ATM* may also be accompanied by tumor-specific lethality in HNSCC cells. Therefore, we introduced five lentiviral shRNA constructs designed to specifically knockdown ATM expression in ciOKC cells and VU-SCC-120. Each shRNA sequence was complementary to a unique part of the *ATM* mRNA sequence. Introduction of the *ATM* shRNAs resulted in a minor inhibition of cell proliferation in ciOKC cells compared to cells transduced with a control construct (ctrl), but proliferation was significantly inhibited in HNSCC cell line VU-SCC-120, ranging from 21% to 90% (Fig. 4B). The maximum window was observed with shRNA *ATM*1. It was at least 8 times more active in the tumor cell line as compared to the ciOKC cells. To check the knockdown, *ATM* expression was analyzed by qRT-PCR and expression levels were compared with the cells transduced with the control construct. Introduction of four of five *ATM* shRNAs resulted in more than 70% downregulation of *ATM* expression levels. Only transduction with *ATM* shRNA number 5 did not result in significant downregulation of *ATM* expression (Fig. 4C).

ATM is a kinase and druggable by kinase inhibitors. To confirm the tumor-specific decrease in cell viability by ATM inhibition, we also subjected ciOKC and HNSCC cells to different concentrations of the commercially available specific ATM inhibitor CP466722. Analysis of cell viability showed that HNSCC cells were more sensitive to the inhibitor compared to the ciOKC cells (Fig. 4D). The

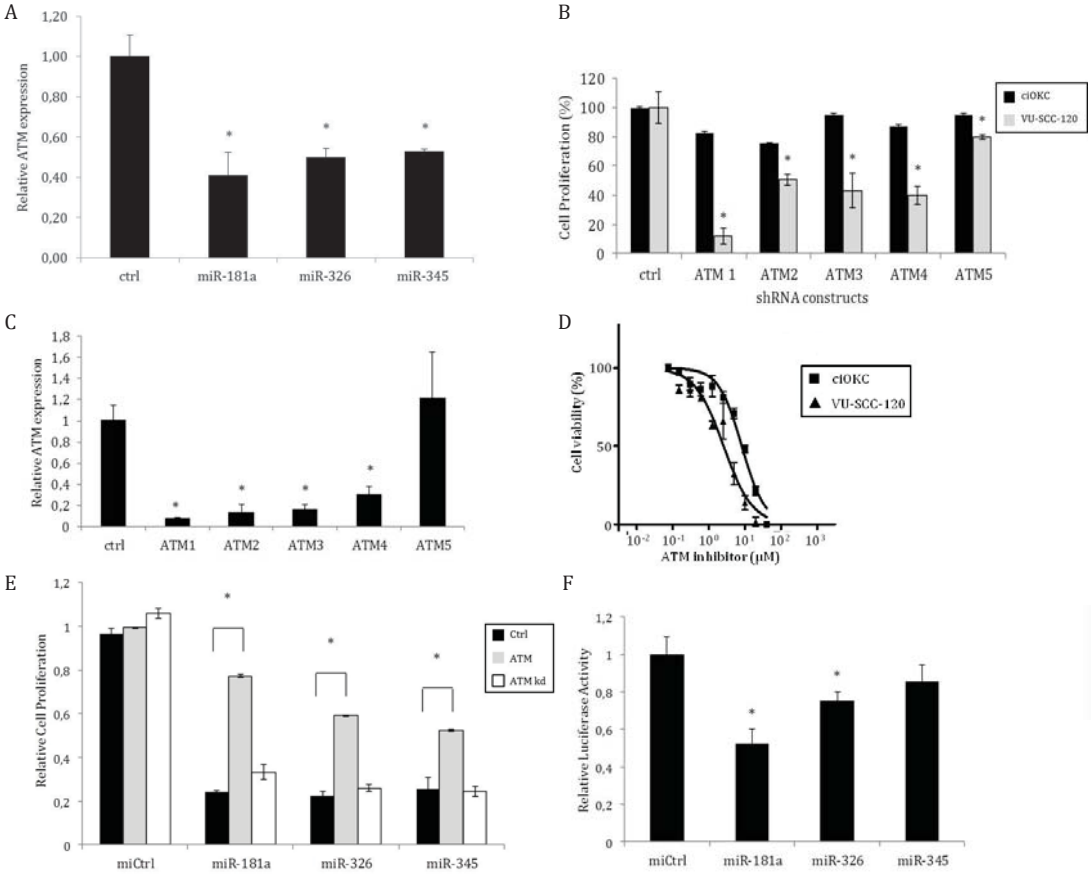

Figure 4. ATM expression is regulated by miR-181a, miR-326 and miR-345 from group A.
(A) Endogenous ATM expression in ciOKC cells was analyzed by qRT-PCR after transient transfection with miR-Vec-Ctrl or the miRNA constructs indicated. In (B) cell proliferation of ciOKC (black bars) and VU-SCC-120 (grey bars) is depicted after ATM knockdown with five different shRNA constructs and control vector (ctrl). In (C) the knockdown of endogenous ATM expression in ciOKC cells is depicted after lentiviral transduction with either a control construct (ctrl) or ATM shRNA constructs 1 to 5. In (D) the sensitivity of HNSCC cell line VU-SCC-120 and ciOKC cells to the ATM drug CP466722 is determined. In (E) rescue experiments with ATM encoding expression constructs are depicted. Wild type ATM (ATM; grey bars) or kinase-dead ATM (ATMkd; white bars) were transfected and the effect on the tumor-selective phenotype of miR-181a, miR-326, miR-345 or miR-Vec-Ctrl (miCtrl) was compared to untransfected cells (ctrl; black bars). In (F) the effect of the miRNAs of group A on ATM 3'UTR luciferase reporter construct is shown. The 3'UTR of ATM was cloned behind the firefly luciferase. Firefly luciferase activity was normalized using Renilla luciferase activity to correct for transfection efficiency. The average of triplicate experiments is shown with standard deviations as error bars. Significant differences are indicated with an asterisk (P <0.05, Student t test).

IC_{50} of 8.2 μM in ciOKC cells shifts to 2.6 μM in VU-SCC-120, a significant change of 3 fold (*P* value <0.05 by *t* testing).
Inhibition of *ATM* by miRNA overexpression, specific *ATM* shRNAs or kinase inhibitors results in a decrease in cell proliferation in HNSCC cells. When *ATM* is the direct effector, ectopic expression of *ATM* should rescue the HNSCC cells from cell death. To investigate this, VU-SCC-120 cells were transfected with either wild type *ATM* (ATMwt) or a kinase-dead mutant *ATM* (ATMkd) in an expression cassette that lacks the 3'UTR of *ATM*. Overexpression of ATMwt or ATMkd was confirmed by qRT-PCR (Supplementary Fig. S4). Next miRNAs miR-181a, miR-326 and miR-345 were introduced in these two cell lines and compared with untransduced VU-SCC-120 (ctrl). The miRNAs all showed a decrease in cell proliferation in the untransduced VU-SCC-120 (Fig. 4E). However, in the cells with the ATMwt expression construct, cell proliferation was rescued up to ~80% (miR-181a) and ~50% (miR-326 and miR-345). Rescue was not observed when

the kinase-dead mutant *ATM* was ectopically expressed in VU-SCC-120 cells. These data indicate that the miRNAs inhibit *ATM* expression, which elicits the tumor-selective lethal phenotype and it depends on the kinase activity of ATM.

Targeting of ATM by miR-181a, miR-326, and miR-345

MiRNAs are known to regulate gene expression post-transcriptionally via binding to the 3'UTR or coding sequences of a mRNA sequence. To demonstrate an effect of miR-181a, miR-326 and miR-345 on the 3'UTR of the *ATM* gene miRNAs were cotransfected with a luciferase reporter construct cloned to the *ATM* 3'UTR sequence. Transfection of ciOKC with miR-181a and miR-326 suppressed the activity of a luciferase reporter gene cloned to the 3'UTR of *ATM*. MiR-345 did show an effect but not significant (Fig. 4F).

The knockdown of *ATM* by the respective miRNAs seems to inversely correlate with the effect of ectopic *ATM* expression. In addition, ectopic *ATM* expression does not rescue the lethal phenotype to 100%. This suggests that some miRNAs might not target the 3'UTR, but also the 5'UTR or coding sequences. These sequences are still present in the expression construct, only the 3'UTR of *ATM* has been substituted. We further hypothesized that another gene target might be involved as well. First, we re-inspected our expression data and found another gene significantly downregulated in 9 of 10 available probes: CD40. We next checked the presence of miRNA target sites using RNA22 and TargetScan on both *ATM* and *CD40*. Multiple binding sites were found for these miRNAs in these genes, albeit mostly not in the 3'UTR region (Supplementary Table S5). The relevance of the various putative miRNA target sites and the role of CD40 and its interaction with ATM requires further elucidation.

DISCUSSION

In the present study, we identified six miRNAs that, when ectopically expressed, lead to a tumor-specific inhibition of proliferation in HNSCC cells, and not in primary keratinocytes. MiRNAs are generally classified into different families based on their sequence homology, most particularly of the seed sequence, and it is hypothesized that different miRNAs within the same family may have similar effects on gene expression. Although all miRNAs highlighted in this study have a tumor-specific lethal effect, and some even recognize at least one identical and apparently critical target gene, they do not belong to the same family.

Many miRNAs have already been implicated in cancer development and progression. For miR-345, a role in head and neck cancer development has been suggested previously by profiling studies. In these studies miRNA expression profiles in tumor samples were compared to normal mucosal epithelium, and it was shown that miR-345 showed an increased expression level in malignant cells[10]. Functional genetic studies showed that miR-181a has tumor-suppressive properties in HNSCCs[15]. Here, we showed a tumor-specific lethal effect for ectopic expression of these two miRNAs as well as miR-326, miR-342, miR-371, and miR-323 in head and neck cancer cells. We also showed that a similar lethal effect was observed when those six miRNAs were introduced in colon cancer and glioblastoma cell lines, although there was a considerable variation in the lethal phenotype between cell lines of different origins. It might therefore be of interest to repeat similar screens in other tumor types. Unfortunately, it is not always possible to have access to matched normal (or near normal) cells, which are required to allow a tumor-specific lethal screen and subsequent validation. Assuming that the identified hits are synthetic lethal with cancer-associated alterations in conserved cellular pathways, such as cell cycle control or DNA repair, the precise source and histotype of the normal reference cells might be less critical, and normal fibroblasts may be sufficient.

MiRNAs regulate gene expression at the post-transcriptional level. One gene may be regulated by multiple miRNAs, but also one miRNA may regulate multiple genes. Consequently, it is difficult to study downstream targets of a certain miRNA, particularly as the target genes may also be

involved in the regulation of expression of other genes. Therefore, it is not surprising that many genes were shown to be significantly differentially expressed when the effect of the six tumor-specific lethal miRNAs was analyzed. Although the expression profiles of the six miRNAs were not similar, it was interesting to observe that two groups could be discriminated. Unfortunately, we could not identify an apparent candidate target gene in group B. Likely multiple repeats of the array analysis in multiple cell lines will be required to define more convincing candidate target genes. The limited sample size combined with the strict FDR correction of the *P* values may have skewed the analyses. Moreover, miRNAs might also influence genes at the translational level, which would necessitate alternative approaches to identify the candidate target genes.

However, in group A several probes for ATM showed significant differences. Using *ATM* 3'UTR luciferase reporter experiments, we showed that both miR-181a and miR-326 seem to directly target the 3'UTR sequence of *ATM*. We could not confirm this for miR-345. We also showed that specific down-regulation of *ATM* via shRNA knockdown elicits a similar tumor-specific lethal phenotype. Although there was a slight toxic effect in the normal squamous epithelial cells, the lethal phenotype observed in HNSCC cell lines was much more severe, and HNSCC cells are more sensitive to the specific ATM inhibitor CP466722. Finally, the tumor-selective phenotype of the miRNAs could be rescued by introduction of an *ATM* expression construct that lacks the 3'UTR of *ATM* itself, while the phenotype could not be rescued by expression of a kinase-dead mutant. Intriguingly, there seemed an inverse correlation between reduction of luciferase activity with the *ATM* 3'UTR and the rescue level when expressing an *ATM* cDNA sequence without the 3'UTR, strongly suggesting that target sites in the coding cDNA sequence are highly relevant as well. When analyzing the potential target sites by RNA22 and TargetScan, a binding site for miR-181a was found in the 3'UTR of *ATM*, but many more in the coding cDNA sequence. Mutation of predicted target sites will be required to proof the relevance of all of them, which will be a major future task. A worrying observation is that the various prediction programs come up with different potential binding sites, hampering a focused approach. Nonetheless, such experiments will be required to establish the ultimate proof of *ATM* targeting by these miRNAs of group A.

We also observed that the rescue level never reaches 100% cell survival. There might be many explanations for this observation, but it suggests that also another target gene might be involved, and we could pinpoint CD40 as a first hint. Additional experiments will be required to prove this and that combined targeted treatment might be of benefit.

Our data thus far suggest that HNSCC cells are depending on ATM signaling for their survival. When *ATM* expression is lost, either by shRNA knockdown or when targeted by a miRNA, the cell is unable to survive, at least under culture conditions. ATM senses DNA damage and phosphorylates CHEK2 which in turn activates p53 by phosphorylation. This route plays a major role in maintaining genome integrity and cell cycle control[25]. Intriguingly, *TP53* is mutated in two of the three HNSCC cell lines tested and *ATM* may have become more critical to organize DNA repair or induce a cell cycle block during S/G2 phase after DNA damage independent of p53. The third cell line UM-SCC-6 is *TP53* wild-type, but it is unclear whether p53 is still functionally active. Detailed analyses of the ATM/ATR-CHEK1/CHEK2 pathway should reveal which critical downstream signaling route causes the lethal phenotype and what the mechanism is. Obviously ATM has many downstream targets, and the tumor-selective phenotype might be related to alterations in other signalling routes. Nonetheless, our data suggest that *ATM* is an interesting drug target for HNSCC.

Previously, it has been shown that miR-181a targets *KRAS*, and this was put forward as an explanation for the observation that this particular miRNA inhibits proliferation of squamous cancer cells[15]. This seemed a little remarkable as *KRAS* mutations are hardly found in HNSCCs, suggesting that this is not the most critical driving gene or even pathway in squamous oncogenesis. Based on our data, we assume that the targeting of *ATM* by miR-181a is the likely event that causes a proliferation stop and cell death in squamous cancer cells.

In summary, we showed here that functional screens by miRNA expression libraries are an

effective way to identify novel druggable targets. We showed that the ectopic expression of miRNAs such as miR-323, miR-345, miR-371, miR-181a, miR-342, and miR-326 may serve as a new treatment in HNSCC. Particularly in head and neck cancer where access to the tumor is relatively easy, introduction of miRNAs, for instance by intratumoral injection combined with electroporation, may be a therapeutic possibility in the future[26]. Also, the application of ATM inhibiting drugs might be a very interesting approach to study in clinical trials specifically focusing on HNSCC.

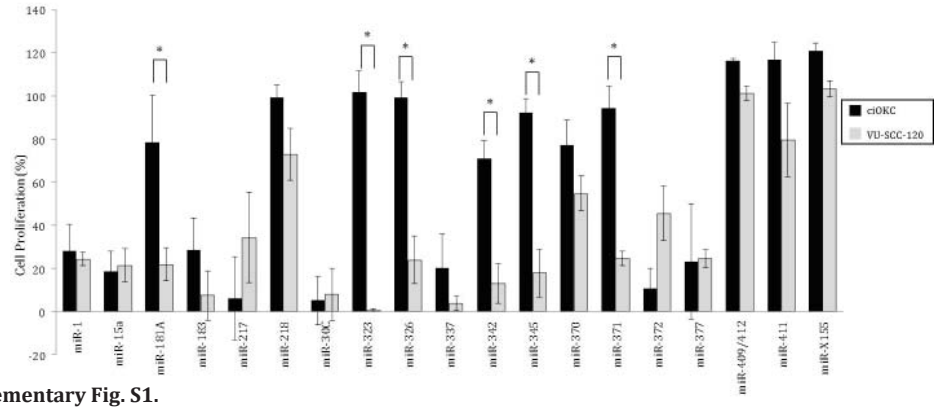

Supplementary Fig. S1.
First validation of the identified 19 microRNAs that seemed to elicit a tumor-selective lethal effect.

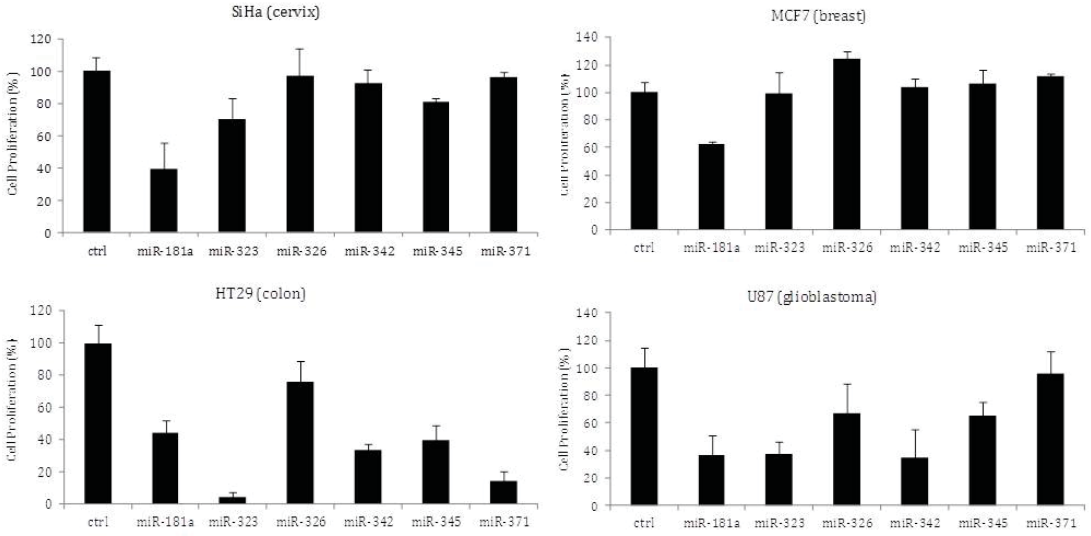

Supplementary Fig. S2.
Effect of the six tumor-selective microRNAs on non-HNSCC cell lines.

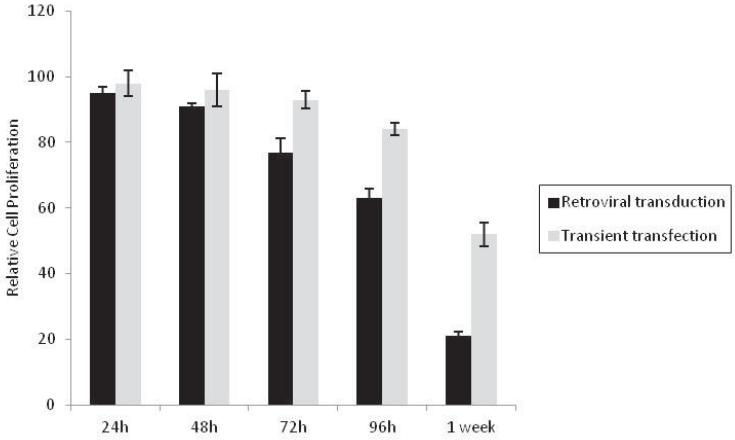

Supplementary Fig. S3.
Phenotypic effect of miR-181a overexpression in time, either when introduced by retroviral transduction or transient transfectionin HNSCC cell line VU-SCC-120.

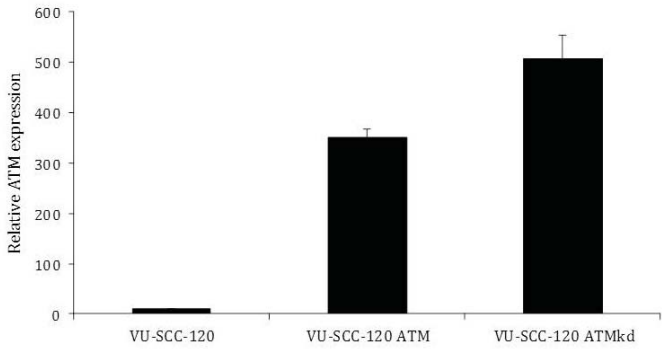

Supplementary Fig. S4.
ATM expression after transient transfection of expression constructs with *ATM* and a kinase-dead *ATM* (ATMkd) mutant lacking the 3'UTR of *ATM*.

Supplementary Table S1. Cell density estimates in screen

Numbers represent the precentage of cell culture confluency and are averages of duplicate experiments. The tumor lethal phenotype is highlighted in grey.

microRNA	ciOKC	VU-SCC-120
miR-15a	75.00	0.00
miR-1	90.00	30.00
miR-30c	75.00	25.00
miR-181a	90.00	25.00
miR-183	85.00	7.50
miR-217	75.00	15.00
miR-218	85.00	30.00
miR-323	85.00	0.00
miR-326	85.00	27.50
miR-345	75.00	0.00
miR-342	80.00	7.50
miR-337	75.00	30.00
miR-370	90.00	2.50
miR-371	90.00	15.00
miR-372	85.00	5.00
miR-377	75.00	5.00
miR-409/412	80.00	8.75
miR-411	85.00	2.50
miR-X155	90.00	27.50
miR-26	25.00	2.50
miR-20	30.00	0.00
miR-19b	30.00	2.50
miR-26b	25.00	10.00
miR-102	25.00	5.00
miR-106	30.00	0.00
miR-107	15.00	0.00
miR-192	20.00	15.00
miR-96	5.00	0.00
miR-135b	20.00	2.50
miR-148b	30.00	0.00
miR-215	20.00	5.00
miR-223	15.00	0.00
BHRF-1	10.00	2.50
miR-145	15.00	0.00
miR-103	3.00	0.00
Let-7f	25.00	0.50
miR-196b	7.50	0.00
miR-424	30.00	0.00
Cand-101 miR-455	25.00	0.00
Cand-216 miR-485	5.50	0.00
Cand-217 miR-485	10.50	0.00
Cand-420	10.50	0.00
Cand-707 miR-193b	10.50	2.50
miR-X56 miR-449a/b	15.00	0.00
miR-124a	5.00	0.00
miR-33	17.50	5.00

microRNA	ciOKC	VU-SCC-120
miR-122a	20.00	3.75
miR-30	17.50	8.75
miR-X111	0.00	1.25
miR-X120 miR-146b	25.00	8.75
miR-X158 miR-452	10.00	17.50
miR-X171 miR-551b	17.50	17.50
miR-X205	7.50	5.00
miR-X223	1.25	0.00
miR-225	0.00	0.00
miR-X226	1.25	1.25
miR-X227	0.00	0.00
miR-X228	0.00	0.00
miR-X230	0.00	2.50
miR-X231	0.00	0.00
miR-X232	0.00	0.00
miR-X233	0.00	0.00
miR-X235	0.00	0.00
miR-X236	0.00	0.00
miR-X237	0.00	0.00
miR-449	7.50	0.00
miR-450	5.00	1.25
miR-485	7.50	5.00
miR-488	6.25	0.00
miR-513	10.00	6.25
miR-514	17.50	6.25
miR-516	10.00	1.25
miR517a	12.50	1.25
miR-518a	30.00	5.00
miR-527	12.50	1.25
miR-487	5.00	0.00
miR-506/507	7.50	6.25
miR-517c	6.25	6.25
miR-518e	10.00	6.25
miR-519d	22.50	6.25
miR-510e	17.50	3.75
miR-520d	8.75	2.50
miR-139	2.50	0.00
miR-142	6.25	3.75
miR-24/189	60.00	40.00
miR-147	60.00	45.00
miR-91	70.00	45.00
miR-34c	55.00	45.00
miR-99b	65.00	65.00
miR-125	60.00	35.00
BART-1	70.00	47.50
Let-7a1	45.00	45.00

Continued: Supplementary Table S1. Cell density estimates in screen

microRNA	ciOKC	VU-SCC-120	microRNA	ciOKC	VU-SCC-120
Let-7b	60.00	62.50	miR-330	80.00	100.00
Let-7d	60.00	70.00	miR-339	85.00	100.00
Let-7e	70.00	45.00	BHRF1-3	75.00	80.00
miR-380	55.00	50.00	miR-146	80.00	100.00
Cand-142	35.00	52.50	Let-7c	85.00	100.00
Cand-181	60.00	65.00	miR-335	75.00	100.00
Cand-350 miR-421	42.50	50.00	miR-337	85.00	100.00
Cand-853 miR-181c/d	45.00	52.50	miR-369	100.00	100.00
miR-126	40.00	32.50	miR-373	90.00	100.00
miR-X119 miR-421	70.00	65.00	miR-361	95.00	97.50
miR-X123 miR-495	60.00	57.50	miR-378	100.00	100.00
miR-X172	57.50	45.00	miR-379	95.00	100.00
miR-X184	33.75	62.50	miR-381	90.00	75.00
miR-X197 miR-542	52.50	57.50	miR-383	90.00	100.00
miR-X248	42.50	60.00	miR-384	95.00	100.00
miR-X249	37.50	47.50	miR-422a	85.00	97.50
miR-X254	45.00	55.00	miR-425	100.00	100.00
miR-X258	55.00	62.50	Cand-35	100.00	100.00
miR-X260	45.00	62.50	Cand-279	80.00	100.00
miR-X261	50.00	52.50	Cand-347 miR-532	80.00	100.00
miR-452	70.00	65.00	Cand-428	80.00	100.00
miR-489	45.00	42.50	miR-X15	80.00	100.00
miR-511	70.00	45.00	miR-X39	75.00	100.00
miR-512	47.50	50.00	miR-X49	75.00	100.00
miR-486	52.50	70.00	miR-X65 miR-448	95.00	90.00
miR-498	57.50	47.50	miR-X86	100.00	100.00
miR-25	100.00	95.00	miR-X87	95.00	100.00
miR-23b	90.00	80.00	miR-X89	100.00	100.00
miR-27b	100.00	85.00	miR-X91	95.00	100.00
miR-29c	100.00	100.00	miR-X98	90.00	100.00
miR-30e	100.00	80.00	miR-X100	95.00	100.00
miR-152	100.00	95.00	miR-X101	85.00	77.50
miR-104/21	85.00	100.00	miR-X102 miR-582	90.00	100.00
miR-196	100.00	100.00	miR-X104	95.00	100.00
miR-197	90.00	90.00	miR-X107	85.00	100.00
miR-198	100.00	100.00	miR-new/208	100.00	95.00
miR-208/new	75.00	100.00	miR-137	90.00	97.50
miR-140	95.00	85.00	miR-138	92.50	90.00
miR-153	100.00	90.00	miR-133	95.00	100.00
miR-186	100.00	100.00	miR-127	100.00	100.00
miR-195	100.00	100.00	miR-99a	100.00	100.00
miR-204	75.00	80.00	miR-29	82.50	82.50
miR-219	100.00	90.00	miR-X110	100.00	92.50
miR-220	100.00	95.00	miR-X112 miR-504	85.00	95.00
miR-221	100.00	90.00	miR-X118	100.00	97.50
miR-224	90.00	90.00	miR-X126	97.50	95.00
miR-299	95.00	90.00	miR-X129	90.00	97.50

Continued: Supplementary Table S1. Cell density estimates in screen

microRNA	ciOKC	VU-SCC-120	microRNA	ciOKC	VU-SCC-120
miR-X130	100.00	100.00	miR-X266	82.50	72.50
miR-X133	85.00	77.50	miR-X267	100.00	87.50
miR-X134	87.50	80.00	miR-X269	80.00	77.50
miR-X136	92.50	90.00	miR-X270	95.00	100.00
miR-X144	85.00	72.50	miR-X271	92.50	87.50
miR-X150	82.50	75.00	miR-432	95.00	92.50
miR-X151	95.00	100.00	miR-448	87.50	87.50
miR-X152	82.50	87.50	miR-453	82.50	87.50
miR-X154	97.50	100.00	miR-490	85.00	100.00
miR-X156	92.50	100.00	miR-491	77.50	95.00
miR-X159	85.00	97.50	miR-492	95.00	97.50
miR-X163	85.00	85.00	miR520e	87.50	82.50
miR-X165	85.00	85.00	miR-24	100.00	55.00
miR-X167	90.00	82.50	miR-98	95.00	70.00
miR-X169	77.50	75.00	miR-19a	85.00	50.00
miR-X170	90.00	100.00	miR-106b	90.00	70.00
miR-X173	95.00	100.00	miR-154	95.00	65.00
miR-X175	95.00	95.00	miR-193	95.00	45.00
miR-X176	90.00	75.00	miR-199a	100.00	50.00
miR-X177	97.50	95.00	miR-200c	75.00	35.00
miR-X179	92.50	95.00	miR-213/181a/181b	80.00	50.00
miR-X181	82.50	72.50	miR-214	85.00	40.00
miR-X182 miR-539	90.00	72.50	miR-296	95.00	70.00
miR-X185	87.50	80.00	miR-320	90.00	55.00
miR-X187	87.50	85.00	miR-328	95.00	70.00
miR-X188	85.00	75.00	miR-331	85.00	70.00
miR-X189	90.00	72.50	miR-144	90.00	70.00
miR-X192	82.50	85.00	miR-376a	80.00	47.50
miR-X194	82.50	72.50	miR-382	80.00	40.00
miR-X196	75.00	87.50	miR-141	92.50	70.00
miR-X201	95.00	80.00	miR-X142	75.00	62.50
miR-X202 miR-487b	75.00	77.50	miR-X147	77.50	65.00
miR-X203	85.00	90.00	miR-X199	72.50	47.50
miR-X204 miR-429	97.50	72.50	miR-X208	80.00	65.00
miR-X210	85.00	82.50	miR-X214	75.00	57.50
miR-X211	87.50	100.00	miR-X239	75.00	57.50
miR-X212	82.50	77.50	miR-X250	80.00	70.00
miR-X215	92.50	85.00	miR-X257	90.00	60.00
miR-X217	95.00	82.50	miR-X262	80.00	37.50
miR-X219	100.00	95.00	miR-X263	72.50	57.50
miR-X222	87.50	97.50	miR-X264	82.50	65.00
miR-X238	87.50	80.00	miR-X268	87.50	47.50
miR-X245	77.50	82.50	miR-32	40.00	0.00
miR-X246	100.00	87.50	miR-22	35.00	0.00
miR-X251	72.50	72.50	miR-23	35.00	0.00
miR-X252	95.00	97.50	miR-16/15a	40.00	2.50
miR-X253	87.50	85.00	miR-17	50.00	2.50

Continued: Supplementary Table S1. Cell density estimates in screen

microRNA	ciOKC	VU-SCC-120
miR-18	47.50	30.00
miR-99	45.00	0.00
miR-97	65.00	0.00
miR-95	55.00	20.00
miR-10b	60.00	0.00
miR-10a	55.00	2.50
miR-9	55.00	0.00
miR-7	40.00	15.00
miR-29b	35.00	0.00
miR-30a	50.00	0.00
miR-30b	45.00	0.00
miR-30d	55.00	0.00
miR-34	50.00	2.50
miR-148	45.00	5.00
miR-150	35.00	0.00
miR-155	60.00	5.00
miR-92	45.00	10.00
miR-93	50.00	0.00
miR-100	40.00	5.00
miR-105	35.00	25.00
miR-199	65.00	20.00
miR-125b	45.00	17.50
miR-128b	55.00	10.00
miR-129	45.00	20.00
miR-130a	50.00	12.50
miR-133b	60.00	5.00
miR-181b	40.00	0.00
miR181c/d	70.00	10.00
miR-182	70.00	7.50
miR-184	40.00	0.00
miR-187	55.00	0.00
miR-190	40.00	0.00
miR-191	45.00	10.00
miR-194	50.00	0.00
miR-199b	45.00	0.00
miR-203	60.00	0.00
miR-205	50.00	0.00
miR-206	40.00	0.00
miR-211	40.00	0.00
miR-216	65.00	20.00
miR-222	65.00	5.00
miR-324	60.00	0.00
BART-2	45.00	0.00
BHRF1-2	60.00	0.00
miR-151	50.00	0.00
Let-7g	55.00	0.00
miR-108	35.00	2.50

microRNA	ciOKC	VU-SCC-120
miR-301	40.00	0.00
miR-302a-d	45.00	5.00
miR-346	60.00	25.00
miR-367	65.00	2.50
miR-368	32.50	2.50
miR-374	40.00	0.00
Cand-209 miR-494	55.00	7.50
Cand-262 miR-499	45.00	0.00
Cand-343 miR-363/92	35.00	5.00
miR-X108 miR-488	50.00	0.00
miR-143	65.00	5.00
miR-134	45.00	20.00
miR-136	57.50	15.00
miR-131	40.00	6.25
miR-101	67.50	16.25
miR-123	47.50	18.75
miR-31	60.00	12.50
miR-X114	45.00	27.50
miR-X135 miR-503	70.00	25.00
miR-X140	47.50	27.50
miR-X146 miR-362	60.00	30.00
miR-X240	70.00	30.00
miR-X241	62.50	12.50
miR-X256	57.50	25.00
miR-524	37.50	10.00
miR-526a	65.00	30.00
miR-519c	40.00	11.25
miR-520c	52.50	20.00
Let-7i	70.00	100.00
miR-130b	70.00	85.00
Cand-219 miR-496	45.00	95.00
Cand-502 miR-452	50.00	100.00
Cand-523	60.00	100.00
miR-X26 miR-410	65.00	100.00
miR-X43	60.00	80.00
miR-135	62.50	72.50
miR-X161	65.00	75.00
miR-523	65.00	77.50
miR-501	70.00	87.50
miR-128	30.00	37.50
miR-X127	25.00	32.50
miR-505	30.00	40.00

Supplementary Table S2. Overview of the predicted target genes for each of the six tumor lethal microRNAs. Genes showed were identified by both TargetScan and DIANA-microT. Results obtained with the seperate programs can be found online.

Group A

hsa-miR-181a				
ACVR2A	DLGAP2	LCORL	PDAP1	SLC9A8
ADAMTS1	DMXL2	LIN7C	PDPK1	SLITRK1
ADAMTSL1	DOCK7	LMO1	PDXDC1	SMAD2
AKAP7	EIF4A2	LMO3	PHACTR2	SS18L1
ANKRD43	ELAVL4	LPP	PI4K2A	ST8SIA4
AP1S3	EN1	LRRK2	PJA2	TARDBP
ARID2	EN2	MAMDC2	PLEKHA3	TBC1D1
ATP11A	ENAH	MAP2K1	PODXL	TBC1D4
ATXN1	ENOX2	MARK1	POU2F1	TBL1X
B4GALT1	EPB41	MBNL2	PPP1CB	TCERG1
BAG4	EPB41L3	MEF2A	PPP1R2	TLL1
BAI3	EPC2	METAP1	PPP2R5E	TMEM64
BNC2	ESR1	MEX3B	PRICKLE2	TNFAIP1
BRD1	ETS1	MFAP3L	PRKCD	TNFRSF11B
BRWD1	FAM105B	MINK1	PTPN9	TNPO1
BTBD3	FAM135A	MTF1	PTPRE	TNRC6B
C13orf23	FBXO33	MTMR12	RAD23B	TOM1L1
C14orf43	FOXK1	MTMR9	RAP1B	TSC22D2
CAPRIN1	G3BP2	MTPN	RBM47	UBE2B
CARM1	GABRA1	MYH10	RCOR1	USP9X
CBX4	GABRA4	NAALADL2	RNF169	VANGL1
CCDC117	GPD2	NEGR1	RNF34	WDFY3
CCNJ	GRB10	NFAT5	ROD1	WHSC1
CDH13	GRIK2	NFIB	RPS6KA3	YOD1
CDON	HAND2	NLK	RPS6KB1	YTHDC1
CDYL	HIC2	NLN	RRP15	YTHDF2
CEP350	HMBS	NOL4	RSPO2	YTHDF3
CHD7	HOXA11	NOTCH2	SCD	ZADH2
CHIC1	HOXC8	NPTN	SCHIP1	ZBTB33
CLIP1	HS2ST1	NR1D2	SEL1L	ZBTB4
CNOT6L	KCNA1	NR2C2	SEPT3	ZCCHC14
CNR1	KCNH8	NR3C1	SEMA3C	ZNF236
CNTN4	KCTD10	NR6A1	SERTAD2	ZNF563
CNTNAP2	KIAA0247	ONECUT2	SH3GLB1	ZNF654
CREBL2	KIAA1244	OTUD4	SHE	
CRIM1	KIAA1715	PAG1	SIN3B	
CTDSPL	KIAA2022	PAK7	SIX2	
CTTNBP2NL	KITLG	PAN3	SLAIN2	
CUL3	KLHDC5	PAPD5	SLC19A2	
DDX3X	KLHL29	PARK2	SLC25A25	
DDX3Y	KLHL5	PAWR	SLC25A37	
DERL1	LARP4	PBX3	SLC35F1	
DIP2B	LBR	PCGF2	SLC38A2	

hsa-miR-326
ANK1
C16orf45
C22orf29
CSNK1G1
FBXO41
FGD3
IGF2BP1
LPHN1
PFKFB4
RHOBTB2
SCN2B
SDC3
SDK2
SH3PXD2A
SLC27A4
SPRYD3
STK35
TREML2
WSCD1

hsa-miR-345
SORT1
SRL
TUB

Group B

hsa-miR-323
HPCAL4
PDPK1

hsa-miR-342
ACVR2B
C20orf11
C22orf29
CA12
CLLU1
ERC1
GDA
KIAA1715
PCGF3
SLC5A3
SYNPO2L

hsa-miR-371
None

Supplementary Table S3. Differentially expressed genes group A - Top 40.
The complete list of differentially expressed genes can be found online.

Probe Name	Gene Name	Systematic Name	chr_coord	Freq	Mean effect G1	pvals G1 ttest	pAdj G1 ttest
A_23_P67411	RSHL1	NM_030785	chr19:50990984-50990925	2	-2.73	3.70E-07	0.01
A_24_P29665	CYCS	NM_018947	chr7:24933308-24933249	3	-0.58	5.28E-07	0.01
A_32_P79152	THC2269537	THC2269537	chr10:13809705-13809764	1	-2.58	1.59E-06	0.01
A_23_P101351	ZNF426	NM_024106	chr19:9500038-9499979	1	-0.26	1.52E-06	0.01
A_24_P318939	ZNF337	NM_015655	chr20:25603624-25603565	2	-0.26	1.71E-06	0.01
A_24_P201973	TEP1	NM_007110	chr14:19905998-19905939	2	-0.97	3.38E-06	0.02
A_23_P385529	POLR3E	AB040885	chr16:22247555-22247614	2	-0.92	3.91E-06	0.02
A_23_P35916	ATM	NM_000051	chr11:107741295-107741354	12	-0.53	3.15E-06	0.02
A_23_P35916	ATM	NM_000051	chr11:107741295-107741354	12	-0.51	3.87E-06	0.02
A_23_P57036	CD40	NM_001250	chr20:44190988-44191047	10	-0.32	3.37E-06	0.02
A_23_P61524	CCDC71	NM_022903	chr3:49175272-49175213	2	1.18	3.70E-06	0.02
A_23_P148600	INE1	NM_003669	chrX:46820986-46821045	2	-0.70	8.01E-06	0.03
A_24_P928415	VPS29	BC032462	chr12:109401967-109401908	3	-0.52	8.14E-06	0.03
A_24_P392082	ENST0000 0361800	ENST0000 0361800	chr2:107990089-107990148	1	-0.13	8.46E-06	0.03
A_24_P941167	APOL6	NM_030641	chr22:34381618-34381677	4	-0.67	9.65E-06	0.03
A_23_P160154	GALE	NM_000403	chr1:23868898-23868839	1	-0.18	1.17E-05	0.03
A_23_P66454	GSDML	NM_018530	chr17:35315681-35315272	1	-0.41	1.33E-05	0.03
A_23_P35916	ATM	NM_000051	chr11:107741295-107741354	12	-0.45	1.45E-05	0.03
A_32_P2807	BC064349	BC064349	chr9:94019335-94019394	1	-0.50	2.33E-05	0.03
A_23_P35916	ATM	NM_000051	chr11:107741295-107741354	12	-0.49	1.79E-05	0.03
A_23_P157838	BC020163	BC020163	chr9:96733993-96733934	1	-0.46	2.44E-05	0.03
A_32_P139196	C13orf25	AB176708	chr13:90803001-90803060	2	-0.42	2.10E-05	0.03
A_23_P40611	TCN2	NM_000355	chr22:29336296-29337897	1	-0.37	2.16E-05	0.03
A_23_P64828	OAS1	NM_002534	chr12:111817181-111817240	1	-0.31	2.38E-05	0.03
A_23_P80048	FER1L4	NR_001442	chr20:33609993-33609934	2	-0.29	2.50E-05	0.03
A_23_P127663	PRRG4	NM_024081	chr11:32831592-32831651	1	-0.21	1.87E-05	0.03
A_24_P344087	REC8L1	NM_005132	chr14:23718947-23719109	1	-0.18	1.94E-05	0.03
A_24_P649327	ENST0000 0382957	ENST0000 0382957	chr15:26256366-26256425	1	-0.14	2.09E-05	0.03
A_23_P209183	GLT25D1	NM_024656	chr19:17554237-17554296	1	-0.11	1.98E-05	0.03
A_23_P16733	RALB	NM_002881	chr2:120763388-120763447	2	0.20	2.44E-05	0.03
A_24_P331373	C22orf13	NM_031444	chr22:23263607-23263548	3	0.71	1.70E-05	0.03
A_24_P255609	ENST0000 0324745	ENST0000 0324745	chr1:47939206-47939147	1	-1.03	2.74E-05	0.04
A_23_P117037	LETMD1	NM_015416	chr12:49740022-49740081	1	-0.11	2.87E-05	0.04
A_23_P368896	SNX12	NM_013346	chrX:70063962-70063903	2	0.38	2.88E-05	0.04
A_23_P109235	RALY	NM_016732	chr20:32127502-32128222	2	-0.12	3.41E-05	0.04
A_23_P57036	CD40	NM_001250	chr20:44190988-44191047	10	-0.26	3.52E-05	0.04
A_32_P64025	A_32_P64025	A_32_P64025	chr17:013867922-013867863	1	-0.24	3.73E-05	0.04
A_23_P76145	ARNTL2	AF256215	chr12:27465419-27465477	3	-0.61	4.37E-05	0.05
A_23_P57036	CD40	NM_001250	chr20:44190988-44191047	10	-0.30	4.29E-05	0.05
A_23_P153372	HSH2D	NM_032855	chr19:16130004-16130063	1	-0.25	4.19E-05	0.05

Supplementary Table S4. Differentially expressed genes group B - Top 40.
The complete list of differentially expressed genes can be found online.

ProbeName	Gene Name	Systematic Name	chr_coord	Freq	Mean effect G2	pvals G2 ttest	pAdj G2 ttest
A_23_P67411	RSHL1	NM_030785	chr19:50990984-50990925	2	-2.81	3.54E-07	0.02
A_32_P79152	THC2269537	THC2269537	chr10:13809705-13809764	1	-2.67	1.27E-06	0.02
A_24_P255609	ENST00000324745	ENST00000324745	chr1:47939206-47939147	1	-1.16	1.48E-06	0.02
A_23_P26976	CHAD	NM_001267	chr17:45897133-45897074	1	-1.10	8.63E-06	0.07
A_23_P201816	CEP350	NM_014810	chr1:176813814-176813873	1	0.15	7.05E-06	0.07
A_23_P48295	CDADC1	NM_030911	chr13:48765503-48765562	2	0.26	1.08E-05	0.07
A_23_P43095	ZFHX4	NM_024721	chr8:77939252-77939311	1	0.26	1.06E-05	0.07
A_24_P237231	SNF1LK	NM_173354	chr21:43661409-43661350	3	-0.60	2.55E-05	0.09
A_24_P933927	LOC646262	XM_929207	chr1:23031757-23030677	1	-0.48	1.62E-05	0.09
A_23_P314024	HLA-F	NM_018950	chr6:29801300-29801941	2	-0.11	2.37E-05	0.09
A_23_P23303	EXO1	NM_003686	chr1:238374758-238374817	10	0.07	2.11E-05	0.09
A_24_P222844	PRPF38B	NM_018061	chr1:108954598-108954657	2	0.10	1.87E-05	0.09
A_32_P224345	CB852269	CB852269	chr8:102750799-102750740	1	0.13	2.52E-05	0.09
A_32_P34522	BC010544	BC010544	chr19:926522-926581	2	0.22	3.08E-05	0.10
A_23_P6963	UBE2E1	NM_003341	chr3:23905638-23905697	2	-0.56	3.72E-05	0.10
A_24_P924697	AK055915	AK055915	chr2:37781102-37781043	1	-0.14	3.93E-05	0.10
A_23_P426292	MAPK14	NM_001315	chr6:36186401-36186460	12	0.13	4.35E-05	0.10
A_23_P82738	RAD54B	NM_012415	chr8:95453591-95453532	11	0.20	4.20E-05	0.10
A_32_P127339	THC2340379	THC2340379	chr2:227525741-227525800	1	-1.74	7.37E-05	0.14
A_32_P95462	THC2411536	THC2411536	chr3:122625987-122626046	1	-0.89	1.59E-04	0.14
A_24_P37887	GPR150	NM_199243	chr5:94982958-94983017	1	-0.65	1.03E-04	0.14
A_23_P17624	TIAM1	NM_003253	chr21:31414542-31414483	1	-0.53	1.31E-04	0.14
A_23_P22499	GNL3L	NM_019067	chrX:54468096-54470019	3	-0.33	1.56E-04	0.14
A_23_P134384	PHF14	NM_014660	chr7:10915739-10915798	2	-0.26	1.28E-04	0.14
A_23_P153372	HSH2D	NM_032855	chr19:16130004-16130063	1	-0.18	1.38E-04	0.14
A_23_P46315	DENND2C	NM_198459	chr1:114837655-114837596	3	-0.15	1.29E-04	0.14
A_23_P1552	CTSC	NM_001814	chr11:87681995-87673419	2	-0.15	1.38E-04	0.14
A_23_P14083	AMIGO2	NM_181847	chr12:45757257-45757198	1	-0.15	6.96E-05	0.14
A_23_P101351	ZNF426	NM_024106	chr19:9500038-9499979	1	-0.13	1.48E-04	0.14
A_24_P418216	A_24_P418216	A_24_P418216	chrX:045248341-045248282	1	-0.11	7.67E-05	0.14
A_24_P63262	RPN1	NM_002950	chr3:129823890-129823831	3	-0.10	1.62E-04	0.14
A_24_P315444	LOC644422	XM_930254	chr17:16460203-16460184	2	-0.10	7.75E-05	0.14
A_23_P310350	CARKL	NM_013276	chr17:3458806-3458747	1	-0.09	8.97E-05	0.14
A_32_P58464	LOC152667	NR_002228	chr4:154206595-154206654	1	-0.08	8.70E-05	0.14
A_32_P106864	AA303143	AA303143	chr18:72201393-72201452	1	0.08	1.38E-04	0.14
A_23_P209360	ENST00000288548	ENST00000288548	chr2:23842960-23843019	1	0.11	1.60E-04	0.14
A_23_P363936	HSPA4L	NM_014278	chr4:129111855-129111914	1	0.15	1.37E-04	0.14
A_23_P25503	FNDC3A	NM_014923	chr13:48681463-48681522	2	0.15	1.05E-04	0.14
A_23_P3215	DTWD1	AF168717	chr15:47714239-47722833	12	0.18	1.00E-04	0.14
A_23_P138805	CHORDC1	NM_012124	chr11:89574752-89574693	1	0.19	1.06E-04	0.14

Supplementary Table S5. Predicted binding sites of microRNAs in ATM using RNA22 and TargetScan.

MicroRNA		Position	Region	Folding energy (Kcal/mol)	Predicted target site	MiRNA sequence	Base-pairing mRNA	Base-pairing miRNA	Base-pairs in putative hetero-duplex	Span of tar-get
hsa_miR_181a	RNA22	3261	CDS	-24	ACCCCTTGCCAATGGAAGATGTT	AACATTCAACGCTGTCGGTGAGT	....((..((.((((..((((((	))))))..)))).)).)..)).	14	23
hsa_miR_181a	RNA22	8223	CDS	-24	GACCTCAGATGGTCAGAAGTGTT	AACATTCAACGCTGTCGGTGAGT	...((((((((((....((((((	))))))....))))))..)))).	16	23
hsa_miR_181a	RNA22	8661	CDS	-27	CCCTCTCTCAGCGAAGTGGTGTT	AACATTCAACGCTGTCGGTGAGT	..(((.(((((((..(.((((((	))))))).)))))..)).))).	17	23
hsa_miR_181a	TargetScan	3525	3'UTR	conserved	AGATTTTAGTACTATTGAATGTA	AACATTCAACGCTGTCGGTGAGT				
hsa_miR_326	RNA22	11825	3'UTR	-23	CTGGAGAACTGTTCAGAATA	CCTCTGGGCCCTTCCTCCAG	(((((((((..(((((((...	..)))))))..)).))))))	15	20
hsa_miR_326	RNA22	4974	CDS	-26	AGCAGGTGGAGGTTCAGAAA	CCTCTGGGCCCTTCCTCCAG	....((.((((((((((..	..)))))))).)))..))..	13	20
hsa_miR_345	RNA22	8218	CDS	-24	TAGGAGACCTCAGATGGTCAGA	GCTGACTCCTAGTCCAGGGCTC	...(((.(((..(((((((((.	.))))))....)))..))))))	15	22
hsa_miR_345	RNA22	6712	CDS	-27	GGACCATTGCACTTCCGTCAGC	GCTGACTCCTAGTCCAGGGCTC	(..((.(((.(((...((((((	))))))....))).)))))..)	15	22
hsa_miR_345	RNA22	9831	3'UTR	-26	GTGAGCGGATCACAAGGTCAGG	GCTGACTCCTAGTCCAGGGCTC	..(((((((((.....((((((.	.))))))....)))).))))	14	22
hsa_miR_345	RNA22	7401	CDS	-27	GGGTTTGTGGCAACTGGTTAGC	GCTGACTCCTAGTCCAGGGCTC	((.((((.(((....((((((((	))))))).....)))))))..)).	16	22
hsa_miR_345	RNA22	4865	CDS	-24	TGTTGTGACTTATTAAGTCAGG	GCTGACTCCTAGTCCAGGGCTC	.(((.(((((.....((((((.	.))))))..))).)).)))...	14	22
hsa_miR_345	RNA22	2121	CDS	-23	GGCTCTTATTCTATCAGTTAGA	GCTGACTCCTAGTCCAGGGCTC	((((((....(((..((((((.	.))))))..)))...)))))).	15	22

REFERENCES

1. Leemans CR, Braakhuis BJ, Brakenhoff RH. The molecular biology of head and neck cancer. Nat. Rev. Cancer 2011;11:9-22.
2. Parkin DM, Bray F, Ferlay J *et al*. Global cancer statistics, 2002. CA Cancer J Clin. 2005;55:74-108.
3. Braakhuis BJ, Snijders PJ, Keune WJ *et al*. Genetic patterns in head and neck cancers that contain or lack transcriptionally active human papillomavirus. J Natl. Cancer Inst. 2004;96:998-1006.
4. Gillison ML, Koch WM, Capone RB *et al*. Evidence for a causal association between human papillomavirus and a subset of head and neck cancers. J Natl. Cancer Inst. 2000;92:709-720.
5. van Houten V, Snijders PJ, van den Brekel MW *et al*. Biological evidence that human papillomaviruses are etiologically involved in a subgroup of head and neck squamous cell carcinomas. Int. J Cancer 2001;93:232-235.
6. Cho WC. OncomiRs: the discovery and progress of microRNAs in cancers. Mol. Cancer 2007;6:60-66.
7. Salmena L, Poliseno L, Tay Y *et al*. A ceRNA hypothesis: the Rosetta Stone of a hidden RNA language? Cell 2011;146:353-358.
8. Fabian MR, Sonenberg NFilipowicz W. Regulation of mRNA translation and stability by microRNAs. Annu. Rev. Biochem. 2010;79:351-379.
9. Baek D, Villen J, Shin C *et al*. The impact of microRNAs on protein output. Nature 2008;455:64-71.
10. Cervigne NK, Reis PP, Machado J *et al*. Identification of a microRNA signature associated with progression of leukoplakia to oral carcinoma. Hum. Mol. Genet. 2009;18:4818-4829.
11. Ramdas L, Giri U, Ashorn CL *et al*. miRNA expression profiles in head and neck squamous cell carcinoma and adjacent normal tissue. Head Neck 2009;31:642-654.
12. Chang KW, Liu CJ, Chu TH *et al*. Association between high miR-211 microRNA expression and the poor prognosis of oral carcinoma. J Dent. Res. 2008;87:1063-1068.
13. Li J, Huang H, Sun L *et al*. MiR-21 indicates poor prognosis in tongue squamous cell carcinomas as an apoptosis inhibitor. Clin. Cancer Res. 2009;15:3998-4008.
14. Cimmino A, Calin GA, Fabbri M *et al*. miR-15 and miR-16 induce apoptosis by targeting BCL2. Proc. Natl. Acad. Sci. U. S. A 2005;102:13944-13949.
15. Shin KH, Bae SD, Hong HS *et al*. miR-181a shows tumor suppressive effect against oral squamous cell carcinoma cells by downregulating K-ras. Biochem. Biophys. Res. Commun. 2011;404:896-902.
16. Guo GS, Zhang FM, Gao RJ *et al*. DNA repair and synthetic lethality. Int. J Oral Sci. 2011;3:176-179.
17. van Zeeburg HJ, van Beusechem V, Huizenga A *et al*. Adenovirus retargeting to surface expressed antigens on oral mucosa. J Gene Med. 2010;12:365-376.
18. Smeets SJ, van der Plas M, Schaaij-Visser TB *et al*. Immortalization of oral keratinocytes by functional inactivation of the p53 and pRb pathways. Int. J Cancer 2011;128:1596-1605.
19. Voorhoeve PM, le SC, Schrier M *et al*. A genetic screen implicates miRNA-372 and miRNA-373 as oncogenes in testicular germ cell tumors. Cell 2006;124:1169-1181.
20. Hermsen MA, Joenje H, Arwert F *et al*. Centromeric breakage as a major cause of cytogenetic abnormalities in oral squamous cell carcinoma. Genes Chromosomes. Cancer 1996;15:1-9.
21. Bremmer JF, Braakhuis BJ, Ruijter-Schippers HJ *et al*. A noninvasive genetic screening test to detect oral preneoplastic lesions. Lab Invest 2005;85:1481-1488.
22. Schmittgen TD and Livak KJ. Analyzing real-time PCR data by the comparative C(T) method. Nat. Protoc. 2008;3:1101-1108.
23. Canman CE, Lim DS, Cimprich KA *et al*. Activation of the ATM kinase by ionizing radiation and phosphorylation of p53. Science 1998;281:1677-1679.
24. Witkos TM, Koscianska EKrzyzosiak WJ. Practical Aspects of microRNA Target Prediction. Curr. Mol. Med. 2011;11:93-109.
25. Shiloh Y. ATM and related protein kinases: safeguarding genome integrity. Nat. Rev. Cancer 2003;3:155-168.
26. Takei Y, Nemoto T, Mu P *et al*. In vivo silencing of a molecular target by short interfering RNA electroporation: tumor vascularization correlates to delivery efficiency. Mol. Cancer Ther. 2008;7:211-221.